

An Error Probability Analysis of Jamming Against Wireless Networks

SaiDhiraj Amuru, Harpreet S. Dhillon, R. Michael Buehrer

Wireless @ VT, Bradley Department of Electrical and Computer Engineering, Virginia Tech

Email: {adhiraj, hdhillon, rbuehrer}@vt.edu

Abstract—In this paper, we analyze jamming against wireless networks from an error probability perspective. Specifically, we investigate the impact of a fixed number of jammers against a network of base stations (BS) or access points (AP). We first derive analytical expressions for the error probability of a victim receiver in the downlink of this wireless network and later study whether or not some recent results related to jamming in the point-to-point link scenario can be extended to the case of jamming against wireless networks.

I. INTRODUCTION

Most studies that are related to jamming attacks at the physical layer only consider the presence of a single node (source-destination pair) and develop optimal jamming strategies, see [1], [2] and references therein. Having gained insights about the jamming behavior in a single victim scenario, the next step is to understand the jamming behavior against networks. Jamming against wireless multi-hop networks has previously been addressed from an optimization perspective in [3]-[5]. All these works model networks as a graph and study the jamming problem with an aim to find the best set of nodes/edges to attack so that the network is disconnected. While these studies indicate which nodes/links to be attacked, they do not address the problem of jamming attacks against wireless networks from a physical layer perspective and don't consider infrastructure networks such as cellular or WiFi. Therefore, in this paper, we address the problem of attacking a wireless network when the jammers are randomly deployed in a given area and how this attack can be realized at the physical layer.

We consider a wireless network comprising of BS or APs that are deployed in an area of interest and investigate the impact of a fixed number of jamming nodes that are deployed within this area. The network performance under the jamming attack is analyzed from the perspective of the downlink of a victim receiver that is accessing this wireless network. The jammers are taken to be randomly deployed since the victim receiver location is typically unknown *a priori*. Further, since the number of jammer nodes is fixed, we model the jammer network using a Binomial point process (BPP) [6].

Using the proposed model, we analyze the jamming performance against the wireless network in terms of the error probability of the victim receiver. We derive analytical expressions for this metric and analyze in detail the jamming impact in the presence of shadowing and fading typically seen in wireless environments. The error probability of the victim receiver can be analyzed by using tools from stochastic geometry when random spatial distributions are considered [7]. However, there is relatively limited work in the literature that performs such an analysis (see [8]-[10]). It is important to note that these works are related to non-jamming scenarios.

A. Contributions

The error probability analysis in this paper is not a straightforward extension of the analysis in [8]-[10] because the system model considered in this paper differs in the following aspects: a) a BPP model for the jammers that attack the victim receiver is considered, b) the effects of shadowing are introduced, and c) a realistic path loss model given by $(1+r)^{-\alpha}$ is considered which is different from the path loss models used in [8]-[10].

In addition to obtaining analytical expressions for the error probability of the victim receiver, we discuss in detail the effect of the various parameters, such as the number of jammers per BS and the network loading on the jamming impact at the victim receiver. We also study the impact of some recent findings related to jamming in a point-to-point link scenario,¹ when analyzing jamming against wireless networks. While extending the analysis in [1] to the case of networks is beyond the scope of this paper, we discuss in detail the behavior of various jamming signals using Monte Carlo simulations.

II. SYSTEM MODEL

We consider a victim wireless network of BSs or APs that are modeled according to a homogeneous Poisson point process (PPP) Ψ of density λ_T on \mathbb{R}^2 [11], [12]. The downlink analysis in this paper is performed at the victim receiver which is assumed to be at the origin. The behavior of this wireless network is studied when it is attacked by a jammer network with N_J jammers that is modeled according to a BPP Ψ_J . The jammers are located on a compact disk of radius R_J centered at the origin denoted by $\mathbb{b}(0, R_J) \subset \mathbb{R}^2$.

The received signal at the victim receiver is given by

$$y = \underbrace{\sqrt{P_T \chi_0} (1+r_0)^{-\frac{\alpha}{2}} h_0 s_0 + \sum_{i \in \Psi \setminus \{0\}} a_i \sqrt{P_T \chi_i} (1+r_i)^{-\frac{\alpha}{2}} h_i s_i}_{i_{agg}(r_0)} + \underbrace{\sum_{i \in \Psi_J} \sqrt{P_J \chi_i^J} (1+d_i)^{-\frac{\alpha}{2}} g_i j_i + n}_{j_{agg}}, \quad (1)$$

where the BSs at distances r_i from the origin send symbols $s_i \in \mathcal{M}$ that are taken from a digital amplitude phase modulated constellation with $\mathbb{E}(|s_i|^2) = 1$. The random variable $\chi_i = \exp(x_i)$ has a log-normal distribution and models the shadowing such that $x_i \sim \mathcal{N}(\mu_\chi, \sigma_\chi^2)$, where μ_χ and σ_χ are respectively the mean and standard deviation of x_i . In (1), h_i indicates a complex Gaussian random variable that

¹In [1], we showed that the optimal jamming signaling scheme against a digital amplitude-phase modulation scheme is not Gaussian signaling and that it depends on the victim signal parameters.

models Rayleigh fading with $\mathbb{E}(|h_i|^2) = 1$. The variables r_0, s_0, χ_0 and h_0 are the respective parameters for the serving BS with which the victim receiver communicates. All other BSs signals are therefore interfering with the serving BS signal to the victim receiver. In (1), a_i is an indicator variable that indicates whether or not the i th BS is active at a given time instant. The interfering BSs independently transmit signals with probability p , also known as the activity factor or the network loading factor [13]. Hence, $a_i = 1$ with probability p and is 0 otherwise.

In (1), $\alpha > 2$ is the path loss exponent. It has been shown in [14], [15] that the commonly used distance-based path loss model $r_i^{-\alpha}$ is inaccurate for smaller values of r_i and that it is used only for analytical tractability. Therefore, in this paper, we use a more realistic model given by $(1 + r_i)^{-\alpha}$ to model the path loss between the i th BS and the victim receiver.

Let $N_{J_c} = \frac{N_J}{\pi R_J^2 \lambda_T}$ indicate the number of jammers per cell (or per BS). The jammers attack the wireless network by sending signals $j_i \in \mathcal{M}_J$, where \mathcal{M}_J is the jammer's signaling scheme. In (1), g_i is a zero-mean complex Gaussian random variable that models Rayleigh fading with $\mathbb{E}(|g_i|^2) = 1$ and χ_i^J models the log-normal shadowing such that $\chi_i^J = \exp(x_i^J)$ and $x_i^J \sim \mathcal{N}(\mu_\chi, \sigma_\chi^2)$. The jammers send signals at a constant power level P_J in order to attack the wireless network. In (1), n is the zero-mean complex additive white Gaussian noise (AWGN) at the victim receiver. Define the reference signal-to-noise-ratio (transmit SNR) as $\text{SNR} = \frac{P_T}{\sigma^2}$ and the reference jammer-to-noise ratio is $\text{JNR} = \frac{P_J}{\sigma^2}$.

We assume that the shadowing is constant over the time of interest and hence the serving BS is selected based on the average signal strength. In other words, shadowing impacts the BS selection but fading does not. Under such conditions, the overall effect of shadowing can be absorbed as a perturbation in the locations of the BSs (recall that the BSs are distributed according to a PPP) if $\mathbb{E}(\chi_i^{2/\alpha}) < \infty$ [16], [17]. When this condition holds true, without loss of generality, a new equivalent PPP with density $\lambda_T \mathbb{E}(\chi_i^{2/\alpha})$ can be defined to model the BS locations [17]. Now, the strongest BS association policy in the original PPP is equivalent to the nearest BS policy association in the transformed PPP without shadowing. Therefore, r_0, s_0 and h_0 in (1) will now represent the parameters of the signal received from the closest BS in the transformed PPP. In what follows, for the ease of notation, we denote $\lambda_T \mathbb{E}(\chi_i^{2/\alpha})$ as λ_T .

Since the BSs are modeled according to a PPP, r_0 is a random variable with probability density function (pdf) equal to $f_{r_0}(\eta) = 2\pi\lambda_T\eta \exp(-\pi\lambda_T\eta^2)$ [10]. In (1), the interference caused by the BSs besides the serving BS i.e., $\Psi \setminus \{0\}$, is denoted by $i_{agg}(r_0)$ and the interference caused by jammers is denoted by j_{agg} . The jammers can transmit either additive white Gaussian noise (AWGN) or any standard modulation scheme to attack the victim [1]. The jamming performance using different types of jamming signals will be discussed in Section IV. A list of notations used is shown in Table I.

III. ERROR PROBABILITY

The maximum likelihood-based demodulator for decoding the symbol s_0 at the victim receiver when the received signal

TABLE I. NOTATIONS USED

Notation	Definition
Ψ, λ_T	PPP network of BSs/APs; density of BSs/APs
Ψ_J, N_J	BPP network of jammers; number of jammers
N_{J_c}	Number of jammers per cell (per BS)
P_T, P_J	Transmit power of BSs, jammers
r_0, h_0, s_0	Distance, channel and symbols of the closest BS/AP
r_i, h_i, s_i	Distance, channel and symbols of the i th BS/AP
a_i, p	Indicator variable; activity factor for interfering BSs
d_i, g_i, χ_i^J, j_i	Distance, channel, shadowing and symbols of the i th jammer
μ_χ, σ_χ	shadowing parameters
α	Power-law path loss exponent

is given by (1) is

$$\hat{s}_0 = \arg \min_{s_0 \in \mathcal{M}} \left\{ \Lambda(\tilde{s}_0) = |y - \sqrt{P_T} h_0 (1 + r_0)^{-\frac{\alpha}{2}} \tilde{s}_0|^2 \right\}. \quad (2)$$

By ignoring the constant energy terms, this expression can be further simplified as

$$\Lambda(\tilde{s}_0) \propto P_T |\Delta_{s_0, \tilde{s}_0}|^2 |h_0|^2 (1 + r_0)^{-\alpha} + 2(1 + r_0)^{-\frac{\alpha}{2}} \sqrt{P_T} \Re(v(r_0) h_0^* \Delta_{s_0, \tilde{s}_0}^*), \quad (3)$$

where $\Delta_{s_0, \tilde{s}_0} = s_0 - \tilde{s}_0$, $v(r_0) = i_{agg}(r_0) + j_{agg} + n$ indicates the total aggregate interference, $\Re(x)$ indicates the real part of the variable x , and x^* indicates the complex conjugate of x .

It is clear that in order to analyze the error probability of the victim receiver, $v(r_0)$ has to be characterized. This entails characterizing the statistics of $i_{agg}(r_0)$ and j_{agg} . In [7], the interference generated by a Poisson network model i.e., $i_{agg}(r_0)$ was shown to be equivalent in distribution to an alpha-stable distribution. This equivalence was exploited in [8] and [9] to explicitly characterize the SINR in a non-jamming scenario (in terms of the signal levels as opposed to power levels that are commonly used to analyze outage probability, see [8], [9] for more details) to evaluate the error probability at a receiver. By using the signal-based formulation as opposed to power level-based formulation, the explicit dependency of the error probability on the modulation schemes employed by the receiver were addressed in [8] and [9]. However, as noted in [6] and references therein, there are no closed form approximations for the interference originating from a Binomial field which is the model used for the jammer network distribution in this paper. Hence, alternate techniques are necessary to analyze the error probability of the victim receiver considered in this paper. Specifically, we use the nearest neighbor approximation (corresponding to the modulation scheme \mathcal{M}) method [10] that provides exact expressions for binary modulations and approximations for higher order modulations. It is also important to note that due to the different system model considered in the current work, the results from [8]-[10] are not applicable.

The following steps are used to obtain the overall average symbol error probability (ASEP):

- 1) The pairwise error probability (PEP) conditioned on r_0, h_0 and the specific realization of the jammer network Ψ_J is first expressed as a function of the aggregate interference $v(r_0)$.
- 2) Then using the Gil-Pelaez transform [18], we obtain the cumulative distribution function for the aggregate interference $v(r_0)$ which is used to obtain the average pairwise error probability (APEP) by averaging over r_0, h_0 and the jammer network statistics i.e., the BPP model.
- 3) Finally, APEP is used to compute the ASEP using the nearest neighbor (NN) approximation corresponding to \mathcal{M} [10].

$$\begin{aligned} \text{APEP} &= \mathbb{E}_{|h_0|, r_0, \Psi_J} [\text{PEP}(\Delta_{s_0, \hat{s}_0}; |h_0|, r_0, \Psi_J)] \\ &= \frac{1}{2} - \frac{1}{\pi} \int_0^\infty E_{r_0} \left\{ \frac{\sqrt{\pi P_T}}{4(1+r_0)^{\frac{\alpha}{2}}} |\Delta_{s_0, \hat{s}_0}| \exp \left[-\frac{P_T |\Delta_{s_0, \hat{s}_0}|^2 |\omega|^2}{16(1+r_0)^\alpha} \right] \Phi_{i_{agg}}(|\omega|; r_0) \right\} \mathbb{E}_{\Psi_J} [\Phi_{j_{agg}}(|\omega|)] \Phi_n(|\omega|) d|\omega| \end{aligned} \quad (7)$$

$$\begin{aligned} \mathbb{E}_{\Psi_J} [\Phi_{j_{agg}}(|\omega|)] &= \left(\frac{1}{|\mathcal{M}_J|} \sum_{j_i \in \mathcal{M}_J} \mathbb{E}_x \left\{ \right. \right. \\ &\quad \left. \frac{1}{R_J^2} \left[{}_1F_1 \left[\frac{-2}{\alpha}; 1 - \frac{2}{\alpha}; -\frac{(|\omega| \sqrt{P_J \chi} |j_i|)^2 (1+R_J)^{-\alpha}}{4} \right] (1+R_J)^2 - {}_1F_1 \left[\frac{-2}{\alpha}; 1 - \frac{2}{\alpha}; -\frac{(|\omega| \sqrt{P_J \chi} |j_i|)^2}{4} \right] \right] \right. \\ &\quad \left. \left. - \frac{2}{R_J^2} \left[{}_1F_1 \left[\frac{-1}{\alpha}; 1 - \frac{1}{\alpha}; -\frac{(|\omega| \sqrt{P_J \chi} |j_i|)^2 (1+R_J)^{-\alpha}}{4} \right] (1+R_J) - {}_1F_1 \left[\frac{-1}{\alpha}; 1 - \frac{1}{\alpha}; -\frac{(|\omega| \sqrt{P_J \chi} |j_i|)^2}{4} \right] \right] \right\} \right)^{N_J} \end{aligned} \quad (9)$$

A. PEP derivation

Let $\mathbb{P}(s_0 \rightarrow \hat{s}_0 | h_0, r_0, \Psi_J)$ indicate the probability with which an error is made in detecting the actual symbol s_0 as \hat{s}_0 . Note that this happens when the likelihood metric is maximized or in other words (2) is minimized at a symbol \hat{s}_0 which is different from s_0 . Mathematically, this can be represented as follows;

$$\begin{aligned} &\mathbb{P}(s_0 \rightarrow \hat{s}_0 | h_0, r_0, \Psi_J) \\ &\stackrel{(a)}{=} \mathbb{P} \left\{ \Re(v(r_0)) < -\frac{(1+r_0)^{-\frac{\alpha}{2}} \sqrt{P_T} |\Delta_{s_0, \hat{s}_0}| |h_0|}{2} \right\} \\ &= F_{v_{Re}} \left[-\frac{(1+r_0)^{-\frac{\alpha}{2}} \sqrt{P_T} |\Delta_{s_0, \hat{s}_0}| |h_0|}{2} \right], \end{aligned} \quad (4)$$

where $F_{v_{Re}}$ indicates the cumulative distribution function (cdf) of $v_{Re} = \Re(v(r_0))$. In the above equation, (a) follows from the fact that conditioned on r_0 , $|h_0|$ and the realization Ψ_J , the aggregate interference $v(r_0)$ is a circularly symmetric random variable. This is because the constellation symbols are equally probable and symmetric, g_i and h_i are circularly symmetric complex Gaussian random variables and χ_i^J is a real random variable. Hence, $v(r_0)$ has the same distribution as $v(r_0) \exp(-j(\theta_0 + \angle \Delta_{s_0, \hat{s}_0}^*))$ ($\angle x$ is the phase of x).

Let Φ_x indicate the characteristic function of a random variable x . By using the Gil-Pelaez transform [10] to express the cdf $F_{v_{Re}}(x)$ as a function of the characteristic function of the aggregate interference and the facts that (i) v is a circularly symmetric random variable which implies that $\Phi_v(|\omega|; r_0) = \Re(\Phi_v(|\omega|; r_0))$, $\Phi_v(|\omega|; r_0) = \Phi_{v_{Re}}(|\omega|; r_0)$ [9], and (ii) $\Phi_{v_{Re}}$ is a real function, we have

$$\begin{aligned} F_{v_{Re}}(v) &= \frac{1}{2} + \frac{1}{\pi} \int_0^\infty \frac{\sin(|\omega|v) \Phi_{v_{Re}}(|\omega|; r_0)}{|\omega|} d|\omega|, \\ \text{PEP}(\Delta_{s_0, \hat{s}_0}; |h_0|, r_0, \Psi_J) &= \\ &\frac{1}{2} - \frac{1}{\pi} \int_0^\infty \frac{\sin \left[\frac{|\omega| (1+r_0)^{-\frac{\alpha}{2}} \sqrt{P_T} |\Delta_{s_0, \hat{s}_0}| |h_0|}{2} \right] \Phi_v(|\omega|; r_0)}{|\omega|} d|\omega|. \end{aligned} \quad (5)$$

Please see the longer version of this paper [19] for more details on the derivation of (5).

The next step is to evaluate $\Phi_v(|\omega|; r_0)$. Since $i_{agg}(r_0)$, j_{agg} and n are independent of each other we have

$$\Phi_v(|\omega|; r_0) = \Phi_{i_{agg}}(|\omega|; r_0) \Phi_{j_{agg}}(|\omega|) \Phi_n(|\omega|). \quad (6)$$

Therefore the APEP can be shown to be given by (7), which follows by using the fact that h_0 is a zero-mean complex Gaussian random variable with unit variance i.e., $|h_0|$ is a

Rayleigh random variable. Thus, we have to first evaluate the characteristic functions of $i_{agg}(r_0)$ and j_{agg} . It is known that $\Phi_n(|\omega|) = \exp(-|\omega|^2/4)$ for a zero-mean, unit variance complex Gaussian random variable. It remains to evaluate $\Phi_{i_{agg}}(|\omega|; r_0)$ and $\mathbb{E}_{\Psi_J} [\Phi_{j_{agg}}(|\omega|)]$.

The characteristic function $\Phi_{j_{agg}}(|\omega|)$ for a given realization of the jammer topology is first evaluated and then averaged over the BPP in order to obtain $\mathbb{E}_{\Psi_J} [\Phi_{j_{agg}}(|\omega|)]$. Specifically, $\Phi_{j_{agg}}(|\omega|)$ can be shown to be

$$\Phi_{j_{agg}}(|\omega|) = \prod_{i=1}^{N_J} \mathbb{E}_{\hat{z}} \left[\cos \left[|\omega| \sqrt{P_J} (1+d_i)^{-\frac{\alpha}{2}} \hat{z} \right] \right]. \quad (8)$$

where $\hat{z} = \Re(z)$ and $z = \sqrt{\chi_i^J} g_i j_i$. Due to a lack of space, we skip the derivation of (8) in this paper. See the longer version of this paper [19] for a complete analysis.

Theorem 1: The characteristic function of the jammer interference as seen at the victim receiver i.e., $\mathbb{E}_{\Psi_J} [\Phi_{j_{agg}}(|\omega|)]$ is given by (9).

Proof: See Appendix.

The error probability is dependent on the jammer's signaling scheme via the term $\mathbb{E}(\hat{z}^{2q})$ given by

$$\mathbb{E}(\hat{z}^{2q}) = \frac{\Gamma(q + \frac{1}{2})}{\sqrt{\pi}} E(\chi^q) \mathbb{E}[|j_i|^{2q}], \quad (10)$$

where q is a non-negative integer and $\Gamma(x)$ is the gamma function.

Remark 1: Any constant modulus signaling scheme will have the same value for $\mathbb{E}(\hat{z}^{2q})$. This indicates that irrespective of the constant modulus-signaling scheme used by the jammer, the error probability at the victim receiver will remain the same. This behavior is due to the fact that the jammer is not aware of the channel g_i and hence cannot compensate for the random rotations introduced by g_i . Therefore, the results in [1] which indicate that modulation-based jamming is optimal, cannot be reproduced in this case. This behavior will be explained via numerical results in Section IV.

Corollary 1: The APEP of the victim receiver when the jammer network uses a zero-mean, unit variance AWGN jamming signal is given by replacing $\mathbb{E}(|j_i|^{2q})$ in (10) with $\frac{2^q \Gamma(q + \frac{1}{2})}{\sqrt{\pi}}$.

Proof: From [21, Eq. 16], it is known that if X is a Gaussian

$$\begin{aligned}
T_1 &= \frac{1}{|\mathcal{M}|} \sum_{s_i \in \mathcal{M}} \pi p \lambda_T (1+r_0)^2 {}_1F_1 \left[\frac{-2}{\alpha}; 1 - \frac{2}{\alpha}; -\frac{(|\omega| \sqrt{P_T} |s_i|)^2 (1+r_0)^{-\alpha}}{4} \right]. \\
T_2 &= \frac{1}{|\mathcal{M}|} \sum_{s_i \in \mathcal{M}} 2\pi p \lambda_T (1+r_0) {}_1F_1 \left[\frac{-1}{\alpha}; 1 - \frac{1}{\alpha}; -\frac{(|\omega| \sqrt{P_T} |s_i|)^2 (1+r_0)^{-\alpha}}{4} \right].
\end{aligned} \tag{13}$$

random variable with mean ν and variance σ^2 , we have

$$\mathbb{E}[(X - \nu)^{2q}] = \sigma^{2q} \frac{2^q \Gamma(q + \frac{1}{2})}{\sqrt{\pi}}. \tag{11}$$

The proof is straightforward using this result.

Remark 2: Corollary 1 states that the theoretical expression for AWGN jamming can be obtained by replacing $\mathbb{E}(|j_i|^{2q})$ in (10) with (11) i.e., instead of averaging over the various modulation symbols that the jammer may use, the averaging is performed over the Gaussian distribution. While it is not easy to explain the AWGN jamming performance by (9) alone, based on the results in [1] it is expected that when the jammer is not aware of g_i , then the jamming performance of any modulation-based jamming and AWGN jamming will be the same. However, when the jammer can compensate for the effects of the fading channel, then the error probability can be significantly increased by using specific modulation schemes.

Corollary 2: The characteristic function of the aggregate interference from the BSs besides the serving BS is given by

$$\Phi_{i_{agg}}(\omega; r_0) = \exp[\pi p \lambda_T r_0^2 - T_1 + T_2], \tag{12}$$

where T_1 and T_2 are shown in (13).

Proof: See Appendix C in [19].

Finally, by using $\Phi_{i_{agg}}(|\omega|; r_0)$ and $\mathbb{E}_{\Psi_J}[\Phi_{j_{agg}}(|\omega|)]$, the overall APEP in (7) can be evaluated irrespective of the signaling schemes used by the BSs and the jammers.

B. Gaussian-Hermite quadrature approximation

In order to evaluate the jammer characteristic function $\mathbb{E}_{\Psi_J}[\Phi_{j_{agg}}(|\omega|)]$, it is necessary to evaluate functions of the form $\mathbb{E}_{\mathcal{X}}[{}_pF_q[a_1, \dots, a_p; b_1, \dots, b_q; f]]$. Since it is computationally intensive to evaluate the integrals of hypergeometric functions, we use the Gaussian-Hermite quadrature (GHQ) approximation [19].

Lemma 1: By using the Gaussian-Hermite quadrature approximation, we have

$$\begin{aligned}
&\mathbb{E}_{\mathcal{X}}[{}_pF_q[a_1, \dots, a_p; b_1, \dots, b_q; f]] \\
&\approx \frac{1}{\sqrt{\pi}} \sum_{n=1}^N w_n p F_q \left[a_1, \dots, a_p; b_1, \dots, b_q; f \exp(\sqrt{2} \sigma_{\mathcal{X}} x_n) \right], \tag{13}
\end{aligned}$$

where w_n and x_n are the weights and roots of the Hermite polynomial [22].

Proof: The proof follows by using the series expansion of the generalized Hypergeometric function ${}_pF_q[a_1, \dots, a_p; b_1, \dots, b_q; f]$ and the GHQ approximation [19].

In Section IV, we show that $N = 10$ terms can closely approximate (13).

C. ASEP Evaluation

ASEP can be upper bounded by using the union bound and APEP as follows:

$$\text{ASEP} \leq \frac{1}{M} \sum_{m=1}^M \sum_{i=1}^{N_m} \text{APEP}(|\Delta_{m,i}|), \tag{14}$$

where M is the total number of equi-probable symbols in the constellation \mathcal{M} , N_m are the total number of neighbors for the m th symbol and $|\Delta_{m,i}|$ is the distance between the m th symbol and its i th neighbor. By using the nearest neighbor approximation (corresponding to \mathcal{M}), ASEP can be approximated as

$$\text{ASEP} \approx \frac{1}{M} \sum_{m=1}^M N_{\Delta_{\min}}^m \text{APEP}(|\Delta_{\min}^m|), \tag{15}$$

where Δ_{\min}^m is the minimum distance between the m th symbol and all its neighbors and $N_{\Delta_{\min}}^m$ is the number of such neighbors that are at a distance of Δ_{\min}^m . For symmetric constellations, where Δ_{\min}^m is the same for all symbols, we have $\text{ASEP} \approx N_{\Delta_{\min}}^{avg} \text{APEP}(|\Delta_{\min}|)$ where $N_{\Delta_{\min}}^{avg} = \frac{1}{M} \sum_{m=1}^M N_{\Delta_{\min}}^m$. For instance, in the case of 16-QAM, we have $N_{\Delta_{\min}}^{avg} = 3$ and $\Delta_{\min} = 2/\sqrt{10}$ (assuming unit-average energy for the modulation scheme). It is important to observe that this method gives exact error probability expression only for binary modulation schemes. We will next present several results that compare these theoretical expressions with Monte-Carlo simulations.

IV. RESULTS AND DISCUSSION

In this section, numerical results are shown in order to validate the theoretical inferences presented earlier and also to shed light on the jamming impact against the wireless network. We use a BS deployment density equivalent to that of an hexagonal grid with 500m inter site distance i.e. $\lambda_T = 2/(\sqrt{3} \cdot 500^2 \text{m}^2)$ [20]. The simulation area is chosen such that an average of 100 active BSs (according to the activity factor p) are present in the wireless network (to avoid edge effects). The path loss exponent α is taken to be 3.7, $\mu_{\mathcal{X}} = 0$ and $\sigma_{\mathcal{X}} = 6\text{dB}$. In order to account for the shadowing in the BS network, using the displacement theorem the effective BS density is taken to be $\lambda_T \exp\left[\frac{2\sigma_{\mathcal{X}}^2}{\alpha^2}\right]$. The radius R_J of the compact disk $\mathbb{b}(0, R_J)$ in which the jammers are distributed according to a BPP depends on λ_T , N_J and N_{J_c} as $\sqrt{\frac{N_J}{\pi \lambda_T N_{J_c}}}$.

As is convention, the power levels considered in the results shown below correspond to transmit SNR and not the received power levels at the victim receiver. Via simulations we observed that for the parameters chosen, the SINR at the victim receiver is typically in the range $[-10, 30]\text{dB}$.

1) *Gaussian-Hermite quadrature approximation to evaluate $\mathbb{E}_{\Psi_J}[\Phi_{j_{agg}}(|\omega|)]$:* We first discuss the Gaussian-Hermite quadrature approximation used in Lemma 1. We compare

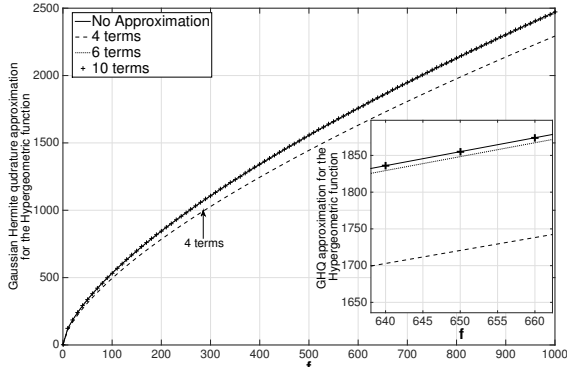


Fig. 1. The accuracy of the Gaussian-Hermite quadrature approximation for error probability evaluation as a function of the number of terms N used in the approximation. The zoomed in plot shows a part of the overall figure and indicates that $N = 10$ terms very closely matches the true value without any approximation.

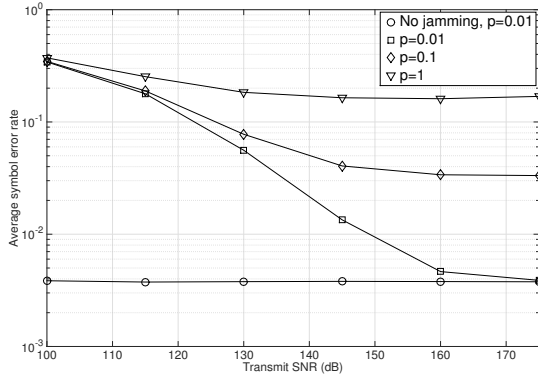


Fig. 2. [Effect of Activity Factor]: Average symbol error rate as a function of the activity factor p when the victim receiver uses BPSK modulation and the jammer network uses BPSK modulation. $N_J = 4$, $N_{J_c} = 1$, $JNR = 100$ dB. The solid lines indicate the Monte Carlo simulation results and the markers indicate the theoretical ASEP evaluated using (14).

$\mathbb{E}_\chi \left[{}_1F_1 \left[-\frac{1}{\alpha}; 1 - \frac{1}{\alpha}; -f\chi \right] \right]$ and $\frac{1}{\sqrt{\pi}} \sum_{n=1}^N w_n {}_1F_1 \left[-\frac{1}{\alpha}; 1 - \frac{1}{\alpha}; -f \exp(\sqrt{2}\sigma_\chi x_n) \right]$ as a function of N when $\sigma_\chi = 6$ dB. The arguments for the Hypergeometric function are chosen based on the jammer characteristic function in Theorem 1. Fig. 1 shows the accuracy of the approximation as a function of N . Since the approximation with $N = 10$ terms closely matches the true value, in what follows we use $N = 10$ and evaluate the error probability.

2) *Effect of number of jammers and activity factor:* Fig. 2 shows the theoretical and the simulation results for the error probability of the victim receiver as a function of the activity factor p when BPSK modulation scheme is used both by the BSs and the jammers. Note that we used BPSK modulation scheme against BPSK victim signal because [1] indicates that BPSK is the optimal modulation scheme against a BPSK victim signal. However replicating the theoretical analysis in [1] to the context of networks is beyond the scope of this paper. Instead, we present various simulation results that take consider various jamming signals that may be used. It is seen in Fig. 2 that the theoretical ASEP expressions in Section III match perfectly with the Monte Carlo simulation results for various activity factors p . Also, ASEP increases with p due to increased interference from the active interfering BSs. The error probability in a non-jamming scenario is constant due to the interference-limited scenarios considered in this paper.

Fig. 3 shows the theoretical and the simulation results

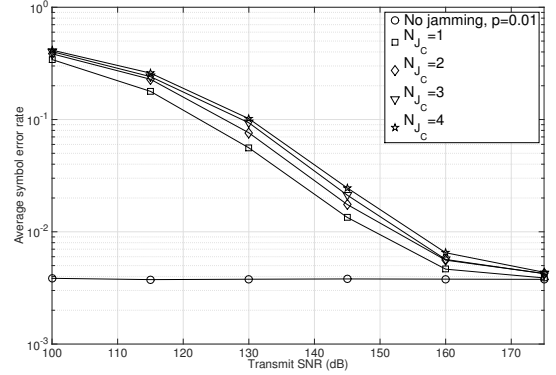


Fig. 3. [Effect of N_{J_c}]: Average symbol error rate when the victim receiver uses BPSK modulation and the jammer network uses BPSK modulation as a function of the number of jammers per cell (BS). The solid lines indicate the Monte Carlo simulation results and the markers indicate the theoretical ASEP evaluated using (14).

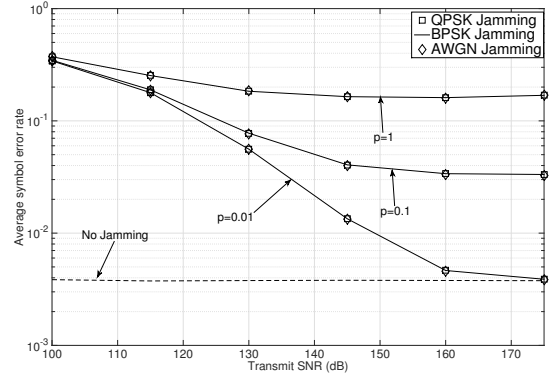


Fig. 4. [Effect of the jamming signaling scheme]: Average symbol error rate as a function of p when the victim receiver uses BPSK modulation and different jamming signals are used by the jammer network. $N_J = 4$, $N_{J_c} = 1$. It is seen that in all cases, the jamming performance of the three jamming signals are the same.

for the error probability as a function of the number of jammers per BS in the network. See that the theoretical and the simulation results match perfectly. Also the behavior of ASEP is as expected—ASEP increases with N_{J_c} due to increased interference from the jammers. Note that because we consider interference limited scenarios, the error probability flattens out in all these results. Further notice that with only one jammer per cell, the error probability can be significantly increased.

3) *Effect of various jamming signals:* Fig. 4 shows the jamming behavior of various jamming signals against BPSK modulated victim signals. As was explained earlier, any constant envelope modulation schemes such as BPSK and QPSK will cause the same impact on the victim. Similarly, the AWGN jamming signal will cause the same error rate at the victim as the jammers are not aware of the fading channel between itself and the victim receiver. Therefore, the random channel g_i between the i th jammer and the victim, randomly rotates the BPSK and QPSK jamming signals which will now appear similar to AWGN signals when they reach the victim receiver. Hence, under such cases the optimal jamming results discussed in [1] are not realized.

Note: In interference limited scenarios, the NN approximation (corresponding to the modulation scheme of the victim) gives exact error probability expressions only for the binary modulation schemes. Under the interference limited scenarios, such as the ones studied in this work, this approximation does

$$\mathbb{E}_{\Psi_J} [\Phi_{jagg}(|\omega|)] = \left[\mathbb{E}_{\hat{z}} \left[\int_{|\omega|\sqrt{P_J(1+R_J)}^{-\frac{\alpha}{2}}}^{|\omega|\sqrt{P_J}} \cos(t\hat{z}) \frac{4}{R_J^2 t \alpha} \left[\frac{|\omega|\sqrt{P_J}}{t} \right]^{\frac{2}{\alpha}} \left[\left[\frac{|\omega|\sqrt{P_J}}{t} \right]^{\frac{2}{\alpha}} - 1 \right] dt \right] \right]^{N_J}. \quad (16)$$

not accurately evaluate the error probability when higher order modulations are considered. Furthermore, we observed that standard computational tools such as Matlab and Mathematica failed in handling singularities in the evaluation of ASEP shown in (14). Despite using the approximations for the hypergeometric functions suggested in [10], we observed that these tools provided significantly different results especially when handling higher order modulations such as QPSK, 16-QAM. It is therefore necessary to find alternative techniques that enable us to analyze higher order modulation schemes as well.

V. CONCLUSION

In this paper, we studied jamming against wireless networks from a physical layer perspective by employing tools from stochastic geometry. Specifically, we studied jamming against a network of BS/AP that are increasingly being modeled according to a PPP. Since the victim locations are typically not known *a priori* we modeled the jammer network with a fixed number of nodes according to a BPP and studied the wireless network performance from the error probability perspective of a victim receiver. We analyzed the error probability of the victim receiver, both from a simulation and a theoretical perspective and showed that the exact error probability expressions can be evaluated in the case of binary modulations. We showed that some recent results related to modulation-based jamming in a point-to-point link setting cannot be directly extended to the case of jamming against wireless networks. Investigating the jammer behavior against higher order modulation schemes and in the case of multiple-input multiple-output-based wireless networks is an interesting future avenue to pursue.

REFERENCES

- [1] S. Amuru and R. M. Buehrer, "Optimal jamming against digital modulation," *IEEE Trans. Inf. Forensics and Security*, vol. 10, no. 10, pp. 2212-2224, Oct. 2015.
- [2] S. Amuru *et al.*, "Jamming bandits," in *arXiv:1411.3652*, Nov. 2014.
- [3] J. Feng *et al.*, "Jammer placement to partition wireless network," in *Proc. Global Commun. Conf. Workshops*, Austin, TX, Dec. 2014, pp. 1487-1492.
- [4] E. Arkin *et al.*, "Optimal placement of protective jammers for securing wireless transmissions in a geographic domain," in *Proc. Intern. Conf. Inf. Proc. Sensor Netw. (IPSN)*, Seattle, WA, Apr. 2015, pp. 37-45.
- [5] P. Tague *et al.*, "Linear programming models for jamming attacks on network traffic flows," in *Proc. Intl. Symp. Modeling and Opt. Mobile, Ad Hoc, and Wireless Netw., (WiOpt)*, Berlin, Germany, Apr. 2008, pp. 207-216.
- [6] S. Srinivasa and M. Haenggi, "Modeling Interference in Finite Uniformly Random Networks," in *Proc. Intern. Workshop on Inf. Theory Sensor Netw. (WITS)*, Santa Fe, NM, Jun. 2007, pp. 1-12.
- [7] M. Z. Win, P. C. Pinto, and L. A. Shepp, "A mathematical theory of network interference and its applications," *Proc. IEEE*, vol. 97, no. 2, pp. 205-230, Feb. 2009.
- [8] M. Di Renzo and W. Lu, "The equivalent-in-distribution (EiD)-based approach: On the analysis of cellular networks using stochastic geometry," *IEEE Commun. Lett.*, vol. 18, no. 5, pp. 761-764, May 2014.
- [9] L. Afify, H. ElSawy, T. Y. Al-Naffouri, and M. S. Alouini, "Error Performance Analysis in Uplink Cellular Networks using a Stochastic Geometric Approach," in *Proc. Intern. Conf. Commun. (ICC) Workshops*, London, UK, 2015.

- [10] M. Di Renzo and P. Guan, "A mathematical framework to the computation of the error probability of downlink MIMO cellular networks by using stochastic geometry," *IEEE Trans. Commun.*, vol. 62, no. 8, pp. 2860-2879, Jul. 2014.
- [11] J. G. Andrews, F. Baccelli, and R. K. Ganti, "A tractable approach to coverage and rate in cellular networks," *IEEE Trans. Commun.*, vol. 59, no. 11, pp. 3122-3134, Nov. 2011.
- [12] H. S. Dhillon, R. K. Ganti, F. Baccelli and J. G. Andrews, "Modeling and Analysis of K-Tier Downlink Heterogeneous Cellular Networks," *IEEE J. Sel. Areas Commun.*, vol. 30, no. 3, pp. 550-560, Apr. 2012.
- [13] H. S. Dhillon, R. K. Ganti and J. G. Andrews, "Load-aware modeling and analysis of heterogeneous cellular networks," *IEEE Trans. Wireless Commun.*, vol. 12, no. 4, pp. 1666-1677, Apr. 2013.
- [14] F. Baccelli, B. Blaszczyzyn, and P. Muhlethaler, "Stochastic analysis of spatial and opportunistic Aloha," *IEEE J. Sel. Areas Commun.*, vol. 27, no. 7, pp. 1105-1119, Sept. 2009.
- [15] H. Inaltekin, M. Chiang, H. Poor, and S. Wicker, "The behavior of unbounded path-loss models and the effect of singularity on computed network characteristics," *IEEE J. Sel. Areas Commun.*, vol. 27, no. 7, pp. 1078-1092, Sept. 2009.
- [16] B. Blaszczyzyn and M. K. Karray, "Quality of service in wireless cellular networks subject to log-normal shadowing," *IEEE Trans. Commun.*, vol. 61, no. 2, pp. 781-791, Feb. 2013.
- [17] H. S. Dhillon and J. G. Andrews, "Downlink rate distribution in heterogeneous cellular networks under generalized cell selection," *IEEE Commun. Lett.*, vol. 3, no. 1, pp. 42-45, Feb. 2014.
- [18] M. Di Renzo, F. Graziosi, and F. Santucci, "On the cumulative distribution function of quadratic form receivers over generalized fading channels with tone interference," *IEEE Trans. Commun.*, vol. 57, no. 7, pp. 2122-2137, Jul. 2009.
- [19] S. Amuru, H. S. Dhillon, and R. M. Buehrer, "On Jamming Against Wireless Networks," available at arXiv:1509.09222, Sept. 2015.
- [20] J. Schloemann, H. S. Dhillon and R. M. Buehrer, "Towards a Tractable Analysis of Localization Fundamentals in Cellular Networks," available at arXiv:1502.06899, Feb. 2015.
- [21] A. Winkelbauer, "Moments and Absolute Moments of the Normal Distribution," in *arXiv:1209.4340*, Jul. 2014.
- [22] M. Abramowitz and I. A. Stegun, "Handbook of Mathematical Functions with Formulas, Graphs, Mathematical Tables." 9th edn, New York, NY, Dover Publications, 1972.
- [23] I. S. Gradshteyn and I. M. Ryzhik, "Tables of Integrals, Series and Products." Academic Press, Elsevier, 2007.

APPENDIX - PROOF OF THEOREM 1

Due to a lack of space, we briefly sketch the proof. For the complete proof, see [19]. The jammer's characteristic function can be shown to be given by (16), which follows by using the fact that the jammers and their locations are independent and identically distributed. To simplify (16), we use [23, Eq. 3.771.4] and then evaluate $\mathbb{E}_{\hat{z}}(\hat{z}^{2q})$. First, recall that $\hat{z} = \Re(z) = \sqrt{\chi}|g_i||j_i| \cos(\angle g_i + \angle j_i)$. Notice that $|g_i| \cos(\angle g_i + \angle j_i)$ is a Gaussian random variable with mean 0 and variance $\frac{1}{2}$. Then by using (11), we have

$$\mathbb{E}_{\hat{z}}(\hat{z}^{2q}) = \frac{\Gamma(q + \frac{1}{2})\mathbb{E}(\chi^q)}{|\mathcal{M}_J|\sqrt{\pi}} \sum_{j_i \in \mathcal{M}_J} |j_i|^{2q}, \quad (17)$$

Substituting (17) in (16), using the series expansion of hypergeometric function and noting that $(\frac{1}{2})_q = \frac{\Gamma(q + \frac{1}{2})}{\sqrt{\pi}}$ and ${}_1F_2[a; b, 1; x] = {}_1F_1[a; b; x]$, we have (9). The expectation of the Hypergeometric functions with respect to χ can be simplified using the GHQ approximation.